O-Linked Sialoglycans Modulate the Proteolysis of SARS-CoV-2 Spike and Contribute to the Mutational Trajectory in Variants of Concern

Edgar Gonzalez-Rodriguez[a,b,1], Mia Zol-Hanlon[a,1], Ganka Bineva-Todd[a,1], Andrea Marchesi[a,b,1], Mark Skehel[c], Keira E. Mahoney[f], Chloë Roustan[d], Annabel Borg[d], Lucia Di Vagno[a], Svend Kjaer[d], Antoni G. Wrobel[e], Donald J. Benton[e], Philipp Nawrath[e], Sabine L. Flitsch[g], Dhira Joshi[h], Andrés Manuel González-Ramírez[m,n,o], Katalin A. Wilkinson[i,j], Robert J. Wilkinson[i,j,k,l], Ramón Hurtado-Guerrero[m,n,o], Stacy A. Malaker[f], and Benjamin Schumann[a,b,*]

[a]Chemical Glycobiology Laboratory, The Francis Crick Institute, NW1 1AT London, United Kingdom; [b]Department of Chemistry, Imperial College London, W12 0BZ London, United Kingdom. [c]Proteomics Science Technology Platform, The Francis Crick Institute, NW1 1AT London, United Kingdom; [d]Structural Biology Science Technology Platform, The Francis Crick Institute, NW1 1AT London, United Kingdom; [e]Structural Biology of Disease Processes Laboratory, Francis Crick Institute, London NW1 1AT, United Kingdom; [f]Department of Chemistry, Yale University, 275 Prospect Street, New Haven, CT, 06511, USA. [g]Manchester Institute of Biotechnology, University of Manchester, 131 Princess Street, Manchester M1 7DN. [h]Chemical Biology Science Technology Platform, The Francis Crick Institute, London NW1 1AT, UK. [i]Tuberculosis Laboratory, the Francis Crick Institute, London, UK. [j]Wellcome Centre for Infectious Diseases Research in Africa, University of Cape Town, Observatory, South Africa. [k]Department of Infectious Diseases, Imperial College London, London, W12 0NN UK. [l]Institute of Infectious Disease and Molecular Medicine and Department of Medicine, University of Cape Town, Observatory, South Africa. [m]Institute of Biocomputation and Physics of Complex Systems, University of Zaragoza, Zaragoza, Spain. [n]Copenhagen Center for Glycomics, Department of Cellular and Molecular Medicine, University of Copenhagen, Copenhagen, Denmark. [o]Fundación ARAID, 50018 Zaragoza, Spain.

S *Supporting Information*

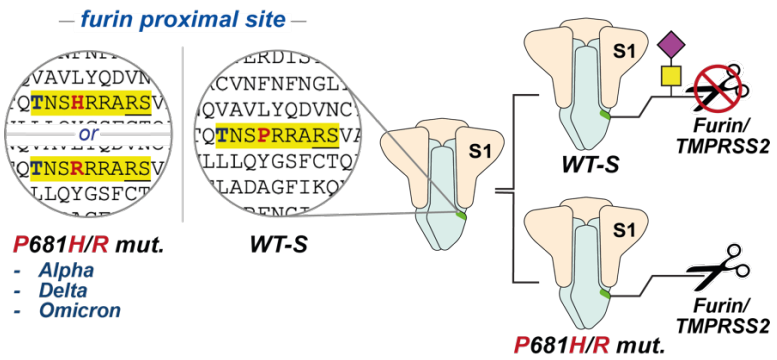

ABSTRACT The emergence of a polybasic cleavage motif for the protease furin in the SARS-CoV-2 spike protein has been established as a major factor for enhanced viral transmission in humans. The peptide region N-terminal to that motif is extensively mutated in major variants of concern including alpha, delta and omicron. Besides furin, spike proteins from these variants appear to rely on other proteases for maturation including TMPRSS2 that may share the same cleavage motif. Glycans found near the cleavage motif have raised questions about proteolytic processing and the consequences of variant-borne mutations. Here, with a suite of chemical tools, we establish *O*-linked glycosylation as a major determinant of SARS-CoV-2 spike cleavage by the host proteases furin and TMPRSS2 and a likely driving force for the emergence of common mutations in variants such as omicron, delta and alpha. We provide direct evidence that the glycosyltransferase GalNAc-T1 primes glycosylation at Thr678 in the living cell. A novel strategy for rapid bioorthogonal modification of Thr678-containing glycopeptides reveals that introduction of a negative charge completely abrogates furin activity. In a panel of synthetic glycopeptides containing elaborated *O*-glycans, we find that

sialic acid moieties reduce furin cleavage rate by up to 65%. Similarly, *O*-glycosylation had a general negative impact on spike cleavage by TMPRSS2, with core 1 (Galβ1-3GalNAc-) *O*-glycan-containing glycopeptides having the largest effect. With a chemistry-centered approach, we thus firmly establish *O*-glycosylation as a major determinant of spike maturation. We propose that a disruption of *O*-GalNAc glycosylation is a substantial driving force for the evolution of variants of concern.

MAIN

The viral surface spike protein has been the subject of intense scientific efforts to understand and curb SARS-CoV-2 transmission.[1–14] Spike is a trimeric, multidomain glycoprotein (**Figure 1a**), with a dense glycan coat that plays crucial structural and immunological roles.[15–28] A key feature in each monomer is an evolutionarily novel arginine-rich peptide sequence initially identified as the cleavage site for the Golgi-located convertase furin. This furin cleavage site (FCS) is crucial for SARS-CoV-2 transmission, as cleavage enhances receptor binding and likely fusion activity of spike.[3,29–31] On a molecular level, furin hydrolyses the peptide bond between Arg685 and Ser686, converting full-length spike (termed FL-S) into the fragments S1 and S2.[7,32–39] Another host protease, TMPRSS2, has been proposed to act synergistically with furin, potentially also targeting the FCS with preference to cleave before arginine.[40,41]

Circulating variants of concern (VOCs) have displayed increased proteolytic processing of spike into S1/S2.[37,42–44] This increase has been associated with a remarkable polymorphism in the peptide stretch preceding the FCS between residues Gln675 and Pro681. Most VOCs and many minor circulating variants carry at least one mutation in that peptide region: alpha and delta display mutations at Pro681 to His and Arg, respectively, whereas all Omicron sub-lineages including BA.1, BA.2 and BA.5 combine P681H with the mutation N679K. Lesser-known variants have featured mutations at Gln675 and Gln677, usually to amino acids with basic functionalities (**Figure 1a**). In line with the cleavage enhancing effect of these mutations, recombinant VOC spike from eukaryotic secretion systems contain much less FL-S than WT spike preparations.[45] While it is tempting to suggest that an increase in basic amino acids enhances furin activity simply due to electrostatic extension of the polybasic cleavage site, this amino acid-centric notion neglects the impact of post-translational modifications. Due to the importance of spike in the viral infectious cycle, the key determinants of processing offer essential insights into the cell biology of viral maturation.

Like most surface proteins on animal viruses, SARS-CoV-2 spike is extensively covered with glycans that impact infection and immunogenicity.[15–28] Among these, Asn (N)-linked glycosylation is straightforward to predict due to the presence of a peptide consensus sequence (N-X-S/T; where X = any amino acid but Pro). In contrast, Ser/Thr-linked *N*-acetylgalactosamine (*O*-GalNAc) glycosylation—which also greatly impacts viral biology—is an analytical challenge due to biosynthetic complexity and the lack of a peptide consensus sequence.[46–56] Notably, the peptide region between Gln675 and Pro681 of SARS-CoV-2 spike harbours multiple Ser/Thr residues that may carry *O*-GalNAc glycans.[19,26,27] Despite the analytical difficulties in understanding *O*-glycan biology, emerging data suggest that *O*-GalNAc glycosylation impacts furin-mediated spike cleavage.[57] Due to the relevance of furin cleavage for viral infectivity, understanding the role of glycosylation in this process is essential.

O-GalNAc glycans are primed by the introduction of the sugar *N*-acetylgalactosamine (GalNAc) into Ser/Thr side chains by a family of 20 GalNAc transferase (GalNAc-T1…T20) isoenzymes. GalNAc-Ts are often associated with isoenzyme-specific, decisive roles in physiological processes that are beginning to be unraveled.[58–67] Understanding the substrate profiles of individual GalNAc-T isoenzymes yields insight into the

regulation of such processes and can be the basis for the development of tools, diagnostics and therapeutics. However, assigning glycosylation sites to individual GalNAc-Ts is challenging due to their complex interplay in the secretory pathway.[68] Analytical profiling of *O*-GalNAc glycoproteins by mass spectrometry (MS) glycoproteomics is further complicated by extension of the initial GalNAc to more elaborated glycans with galactose (Gal), *N*-acetylglucosamine (GlcNAc) and the acidic monosaccharide *N*-acetylneuraminic acid (Neu5Ac) as a capping structure. Indirect methods are thus often used to establish links between GalNAc-T isoenzymes and the glycosylation sites they modify, yielding insights into *O*-glycan biology.[58,69–72] Through lectin staining and co-expression of individual GalNAc-Ts with spike, Ten Hagen and colleagues found seven isoenzymes that introduce GalNAc into spike.[73] Furthermore, co-expression of spike with GalNAc-T1 decreased furin cleavage, suggesting that glycosylation may modulate furin cleavage and, by implication, viral infectivity. These findings corroborate earlier reports suggesting modulation of furin cleavage by *O*-GalNAc glycans in other secreted proteins,[74–78] pointing to a potential additional regulatory switch brought about by *O*-glycans. However, the biosynthetic complexity and technical challenges associated with *O*-glycoproteome analysis have thus far prevented closer investigation. Specifically, we currently lack knowledge on glycan abundance, precise attachment site(s), structural influence on proteolysis and the roles of VOC mutations on *O*-GalNAc glycosylation.

Chemical tools have provided an insight into glycobiology that is orthogonal to classical methods of molecular biology by allowing a direct view into the details of glycan biosynthesis. For example, by using a tactic termed “bump-and-hole engineering”, we have developed a chemical reporter strategy for the activities of individual GalNAc-T isoenzymes in the living cell (**Figure 1b**).[79,80] Through structure-based design, the active site of a GalNAc-T isoenzyme was expanded by mutagenesis to contain a “hole” that is complementary to a “bump” in a chemically modified version of the substrate uridine diphosphate (UDP)-GalNAc.[80] The bumped substrate “UDP-GalN6yne” contained a bioorthogonal alkyne tag that allowed for covalent attachment of fluorophores or biotin after transfer to a glycoprotein, thus unraveling substrates of individual GalNAc-Ts.[80–82] Importantly, UDP-GalN6yne can be biosynthesized in the living cell through the introduction of an artificial metabolic pathway, allowing for the installation of a fully functional GalNAc-T bump-and-hole system.[80,83] Additionally, we recently, we introduced a clickable, positively charged imidazolium tag (termed ITag) that increased the charge state and improved fragmentation-based sequencing of glycopeptides, leading to enhanced MS-based analysis.[84] Building on the power of our chemical tools to dissect the role of *O*-GalNAc glycosylation, we sought to unveil the molecular details of glycan-mediated modulation of spike processing.

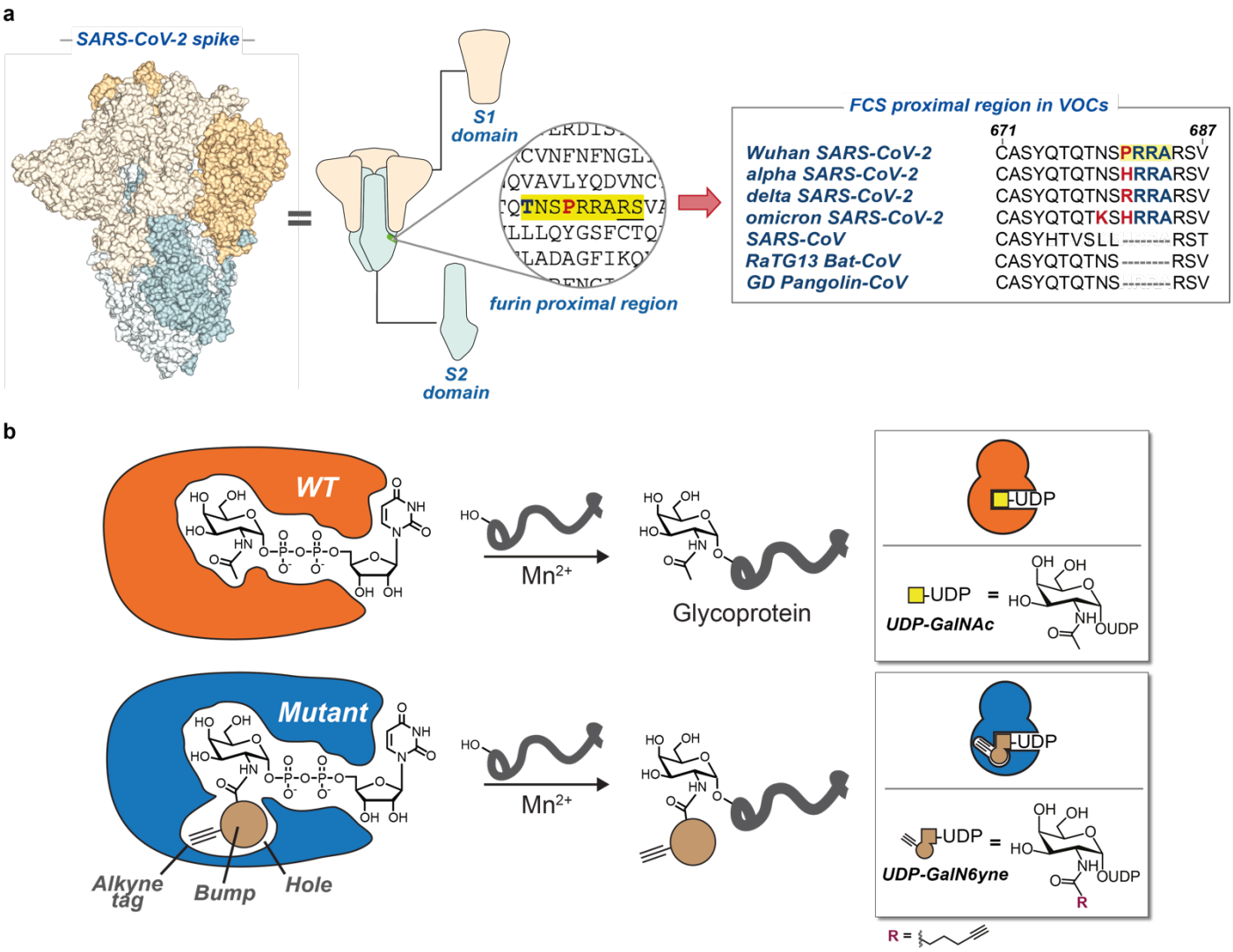

Figure 1. a) SARS-CoV-2 spike model and cartoon. Furin cleavage site and a peptide alignment for COVID-19 variants of concern and related coronaviruses. Highlighted in yellow is the polybasic motif of SARS-CoV-2. Bold and red are amino acid changes in positions 679 and 681. **b)** Bump-and-hole engineering allows for GalNAc-T isoenzyme-specific tagging of glycosylation substrates using the clickable substrate UDP-GalN6yne. FCS = furin cleavage site; VOCs = variants of concern.

RESULTS AND DISCUSSION

Establishing a protein as a GalNAc-T substrate usually requires co-expression with the respective GalNAc-T and detection by GalNAc-recognizing lectins.[73,85] While insightful, such indirect detection rarely provides the identity of the modified glycosylation site and is generally complicated by the interplay between isoenzymes. Bump-and-hole engineering introduces a GalNAc analogue that can be directly related to the respective GalNAc-T but additionally can be tagged by bioorthogonal chemistry and detected by various analytical techniques. We incubated recombinant SARS-CoV-2 spike WT, P681R or P681H constructs produced in human Expi293-F cells with either WT- or BH-versions of GalNAc-T1 (BH = I238A/L295A double mutant) or T2 (BH = I253A/L310A double mutant) and the bumped nucleotide-sugar UDP-GalN6yne. We then tagged glycosylation by Cu(I)-catalyzed azide-alkyne cycloaddition (CuAAC) with clickable biotin and

visualized via Streptavidin blot (**Figure 2a**). A single, highly intense band corresponding to the S1 fragment was observed when WT (Wuhan) spike was incubated with BH-GalNAc-T1 (**Figure 2b**). Note that the glycosylated Thr residues close to the protease cleavage site are located in S1 (see also below for further details). Incubation with BH-T2 or the corresponding WT-GalNAc-Ts led to negligible signal. A single mutation of Pro681 to either His or Arg led to near-complete abrogation of glycosylation by BH-T1. These data suggest that purified, and hence pre-glycosylated, WT-S1 contains a dedicated GalNAc-T1 glycosylation site that is not present in purified FL-S and obstructed upon mutation of Pro681 as seen in common variants.

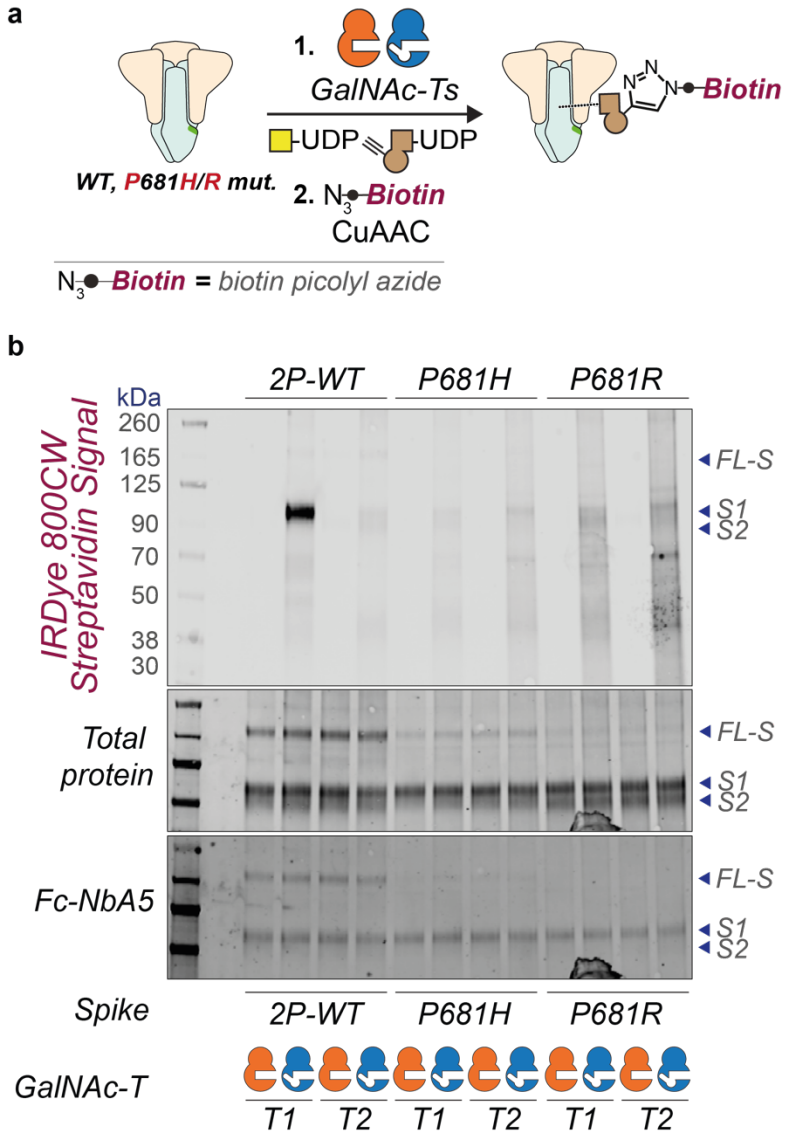

Figure 2. a) Overview of the *in vitro* spike glycosylation/biotinylation experiments. **b)** Streptavidin blot of *in vitro* glycosylated recombinant WT and P681-mutant SARS-CoV-2 spike treated with biotin-azide under CuAAC conditions. FL-S: Full-length spike; Fc-NbA5: mouse-Fc conjugated SARS-CoV-2 RBD spike-specific nanobody.

We then used a panel of synthetic peptides to study the effect of spike mutations on GalNAc-T1-mediated glycosylation (**Figure 3a**). We included peptides with variant-related mutations at the major hotspots: Gln675, Gln677, Asn679 and Pro681. GalNAc-T1 generated both mono- and di-glycopeptides from a WT (Wuhan) substrate peptide (**Figure 3b**). Single mutations at positions 675, 677, and 679 reduced the amount of di-glycosylation but largely retained mono-glycosylation. In contrast, the combination of two mutations at

positions 675 and 677 showed a critical reduction of glycosylation. This was evidenced by reactions with double mutants Q675H+Q677H and Q675H+Q677R where only 9.7% and 5.7% conversions were achieved, respectively. Consistent with the work by Ten Hagen and colleagues,[73] notable reductions in glycosylation were also observed for P681H and P681R peptides, where conversions to glycosylated products were 20.3% and 9.6%, respectively, validating the importance of a Pro in position +3 for GalNAc-T1 glycosylation.[86] These data confirmed the dependence of GalNAc-T1 on Pro681 but suggest that additional nearby mutations, such as those in Omicron (N679K P681H), may have cumulative effects. Mass spectrometry with electron-transfer dissociation (ETD) fragmentation revealed that mono-glycopeptides are exclusively GalNAc-modified on Thr678 while di-glycopeptides are modified at Thr676 and Thr678, pointing to a hierarchy of sites where Thr678 is glycosylated first (**Figure 3c** and **Supporting Figure 1**). When BH-engineered GalNAc-T1 and UDP-GalN6yne were used in the *in vitro* assay with WT spike-derived peptides, the same trends were seen, confirming that BH-T1 recapitulates the substrate specificity of WT-T1 (**Figure 3c** and **Supporting Figure 1**).

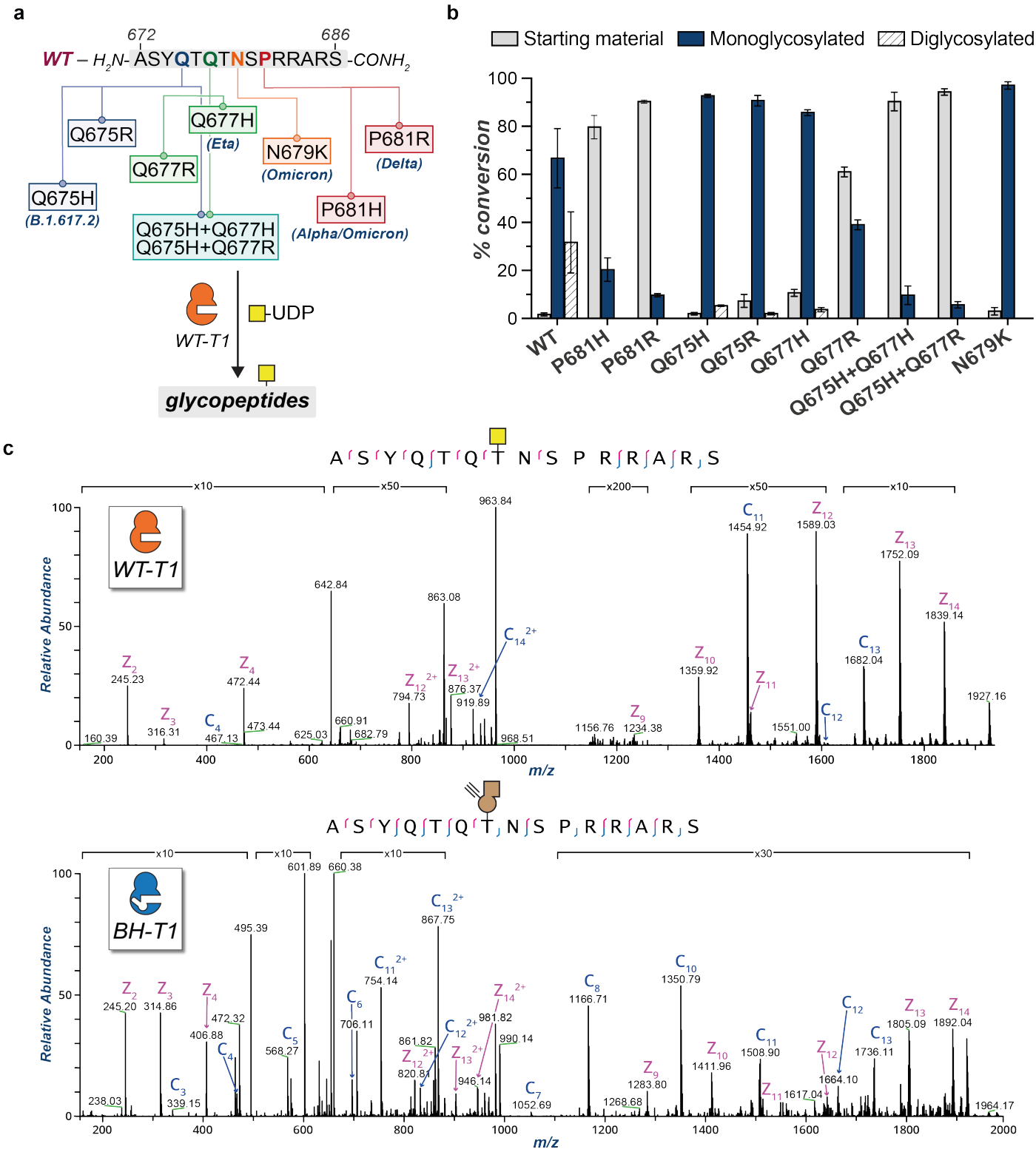

Figure 3. a) Synthetic peptide panel depicting the FCS proximal region of spike in WT and relevant mutants. **b)** *In vitro* glycosylation results with WT-GalNAc-T1 and UDP-GalNAc assessed by LC-MS. **c)** Tandem MS (ETD) spectra for WT and BH-T1 *in vitro* glycosylation of the WT peptide H-ASYQTQTNSPRRARS-NH_2. Synthetic peptides were run on an Orbitrap Eclipse (Thermo) and subjected to ETD, followed by manual validation and hand curation.

GalNAc-T selective MS-glycoproteomics analysis allows *O*-glycosite and glycan composition investigation *in vitro* and in engineered cells

Assigning glycosylation sites to GalNAc-T isoenzymes is complicated by the redundancy of GalNAc-Ts and the complexity of the secretory pathway that is not accurately recapitulated with synthetic peptides. Furthermore, the FCS-adjacent region lacks cleavage sites of most proteases commonly used in MS, resulting in the generation of large glycopeptides and further hampering analysis. Chemical tools can address these shortcomings and report on GalNAc-T activity in the secretory pathway of living cells while offering a bioorthogonal handle to aid MS analysis. We stably transfected Expi293 cells with both SARS-CoV-2 spike (Wuhan) and either WT- or BH-versions of GalNAc-T1 or T2, along with the biosynthetic machinery to generate UDP-GalN6yne in the cell from a readily available precursor (**Figure *4*a**).[87] Spike samples containing alkyne-tagged or control glycans were isolated and derivatized by CuAAC with an azide-functionalized imidazolium group (ITag-azide).[84,88–90] This treatment introduced GalN6yne in an isoenzyme-specific fashion while endowing glycopeptides with an additional permanent positive charge that facilitates MS-analysis.[84] FL-S and S1/S2 fractions were separately subjected to in-gel digestion and analyzed by tandem MS. We used high intensity collision-induced dissociation (HCD) obtain naked peptide sequences and glycan compositions, and then used the ITag-containing GalN6yne diagnostic ion to trigger ETD fragmentation of the peptide backbone (**Figure *4*b**).[56,84,91,92] Through both computational (Byonic, ProteinMetrics) and manual validation, we found Thr678 to carry ITag-modified GalN6yne in both FL-S and S1 samples only in cells expressing BH-T1, but neither BH-T2 nor any WT GalNAc-Ts (**Figure 4c**). The additional positive charge brought about by the ITag permitted straightforward ETD fragmentation of a 21-amino acid glycopeptide. The corresponding glycopeptide in samples expressing WT-T1 could not be unambiguously sequenced, highlighting the ability of chemical tools to help advance site-specific *O*-glycoproteomics. We further found that both BH-T1 and BH-T2 glycosylated Thr323, a previously described glycosylation site that had not been associated with any GalNAc-T isoenzyme (**Figure 4c** and **Supporting Figure 2**). These results were also recapitulated *in vitro* through glycosylation of recombinantly expressed spike with soluble versions of BH-GalNAc-T1 and BH-GalNAc-T2, CuAAC with ITag-azide and MS-glycoproteomics analysis (SI and **Supporting Figure 3**).

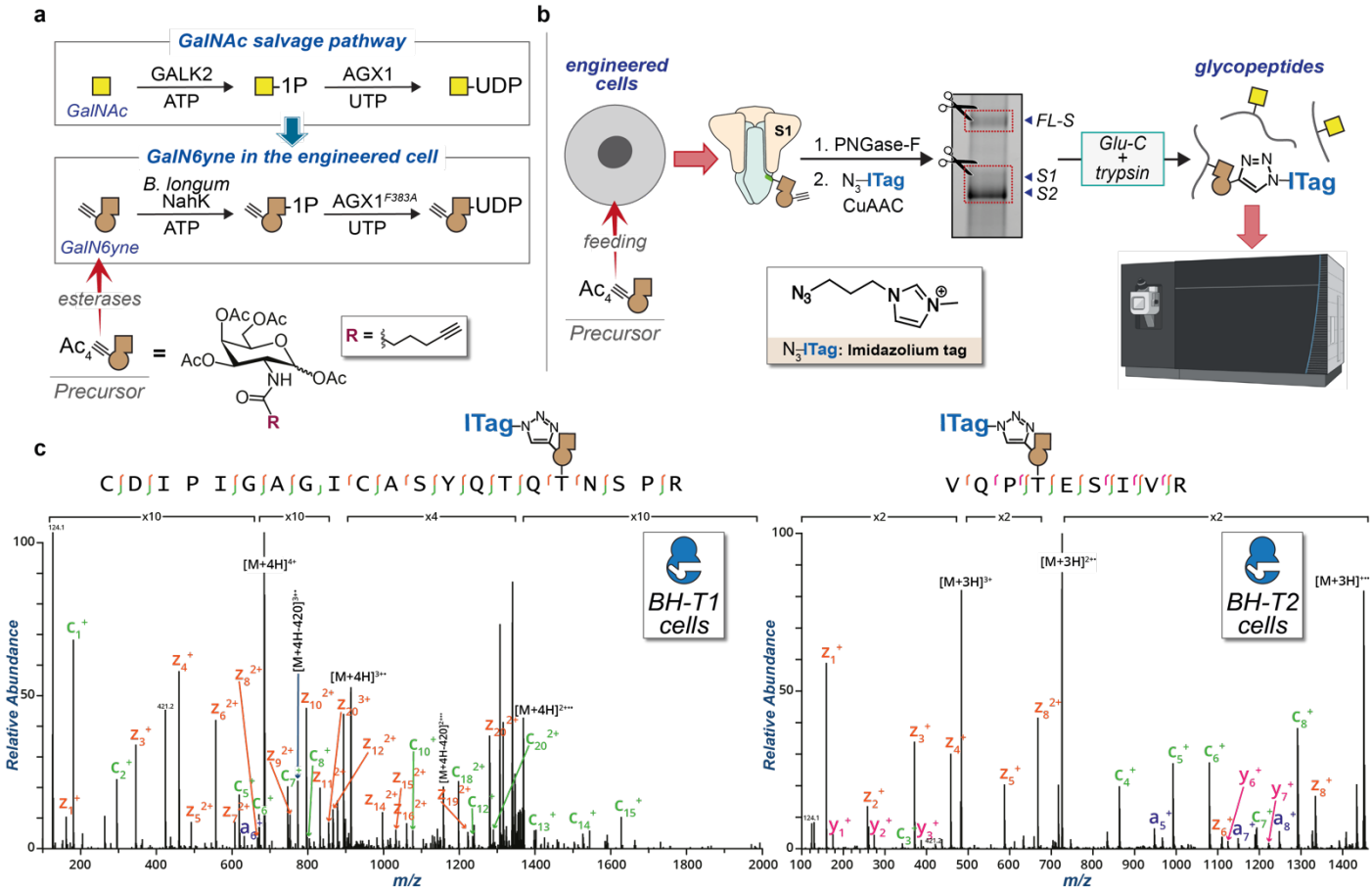

Figure 4. a) GalNAc salvage pathway and its bumped-sugar analogue (GalN6yne) counterpart in engineered cells. Expression of the kinase NahK and the pyrophosphorylase AGX1^{F383A} affects biosynthesis of UDP-GalN6yne in live cells. **b)** Graphical representation of the MS-glycoproteomics methodology for engineered cells. Spike was recombinantly expressed in Expi293 cells expressing BH-GalNAc-Ts, NahK and AGX1^{F383A}. Following isolation and de-N-glycosylation, ITag-azide was introduced by CuAAC and the protein preparation subjected to in-gel digest and tandem MS. **c)** Annotated tandem MS (ETD) spectra of the major hits tagged by BH-GalNAc-T1 (left) and BH-GalNAc-T2 (right).

Elaborated O-linked sialoglycans confer proteolytic resistance to SARS-CoV-2 spike

Glycosylation has the potential to modulate proteolytic processing depending on the distance to the cleavage site and glycan composition.[74,77,78] We directly probed whether *O*-GalNAc glycans on Thr678 modulate cleavage by furin. To this end, we used synthetic Förster Resonance Energy Transfer (FRET)-active substrate peptides to assess proteolytic activity. Peptides spanning residues 672 to 689 contained N-terminal 2-aminobenzoyl and C-terminal 3-nitro-Tyr as fluorescence donor and quencher moieties, respectively. An increase in fluorescence intensity indicated cleavage (**Figure 5a**).[93] We first compared non-glycosylated substrates corresponding to either WT (**FRET-1**) and P681H mutant spike (**FRET-2**). The P681H mutation had no discernable effect on the rate of furin-mediated cleavage, suggesting that the addition of a basic amino acid is not a defining characteristic of furin cleavage enhancement in existing variants of concern.

We hypothesized that an increase of furin rate in mutant spike may not directly stem from recognition of the peptide sequence but rather a decreased capacity of GalNAc-T1 to introduce *O*-GalNAc glycans. We thus tested whether glycosylation of furin substrate-peptides impacts cleavage. FRET reporter peptides carrying GalNAc (**FRET-3**) or alkyne-containing GalN6yne (**FRET-4**) were synthesized by glycosylation with WT- and BH-GalNAc-T1, respectively. Glycosylation with these monosaccharides alone did not substantially impact the furin cleavage rate compared to the WT peptide **FRET-1** (**Figure 5c** and **Supporting Figure 4**). We speculated that elaboration of GalNAc to larger or charged glycans might introduce additional structural constraints on furin recognition but refrained from synthesizing the corresponding glycopeptides at this stage due to the sheer number of potential glycans. The alkyne tag on GalN6yne presented an opportunity to modify the biophysical properties of glycopeptides in a straightforward fashion, allowing more targeted synthetic efforts. We reacted glycopeptide **FRET-4** with two structurally different organic azides under CuAAC conditions: 6-azido-6-deoxy-glucose gave a pseudodisaccharide in **FRET-5**, while 3-azido-propionic acid introduced an additional acidic functionality to test the impact of a negative charge on furin cleavage in glycopeptide **FRET-6**. Both modified glycopeptides displayed a significant reduction in furin cleavage (**Figure 5c** and **Supporting Figure 4**). Steric expansion in **FRET-5** led to 80% decrease in the rate of furin cleavage with respect to **FRET-1**. Strikingly, **FRET-6** which carried a small, negatively charged modification displayed a 93% rate reduction, almost completely abrogating furin activity. We concluded that the elaboration of *O*-glycans on Thr678, especially with negatively charged modifications, severely hampers the activity of furin.

Sialic acid is negatively charged under physiological pH and a common component of *O*-glycans. We reasoned that the presence of sialic acid might modulate furin cleavage, and chemoenzymatically synthesized a set of novel, spike-derived glycopeptides to test on our cleavage assay. First, *Drosophila melanogaster* C1GALT1 was used to extend **FRET-3** with β3-linked galactose to give **FRET-7**.[94] α2,6-Linked sialic acid was introduced into **FRET-3** and **FRET-7** using the enzymes ST6GALNAC1 and ST6GALNAC2, respectively, to yield sialoglycopeptides **FRET-8** and **FRET-9** (**Figure 5d** and **Supporting Figure 5**).[95] While the uncharged disaccharide in **FRET-7** had only a marginal (3.5%) effect on furin rate compared to the parental peptide **FRET-1**, the presence of sialic acid led to a striking 45% reduction of furin rate in glycopeptide **FRET-8** and a 65% reduction in glycopeptide **FRET-9** (**Figure 5e**). We concluded that the elaboration of *O*-glycans on Thr678, especially with negatively charged sialic acid residues, severely hampers furin activity.

To our knowledge, in contrast to furin,[74] TMPRSS2 has never been probed for cleavage of glycopeptide substrates. We sought to establish whether *O*-GalNAc glycans could modulate TMPRSS2 activity in a similar fashion to furin. Recombinant TMPRSS2 was subjected to our selection of (glyco-)peptide FRET substrates **FRET-1**, **FRET-3** and **FRET-7** to **FRET-9** (**Figure 5e**). All glycans somewhat impacted TMPRSS2 activity with respect to the non-glycosylated peptide **FRET-1** regardless of elaboration, with the core 1 (Galβ1-3GalNAc-) glycopeptides **FRET-7** (45% rate reduction) and **FRET-9** (70% rate reduction) impacting cleavage more drastically than their non-galactosylated counterparts **FRET-3** (19% rate reduction) and **FRET-8** (15% rate reduction), respectively.

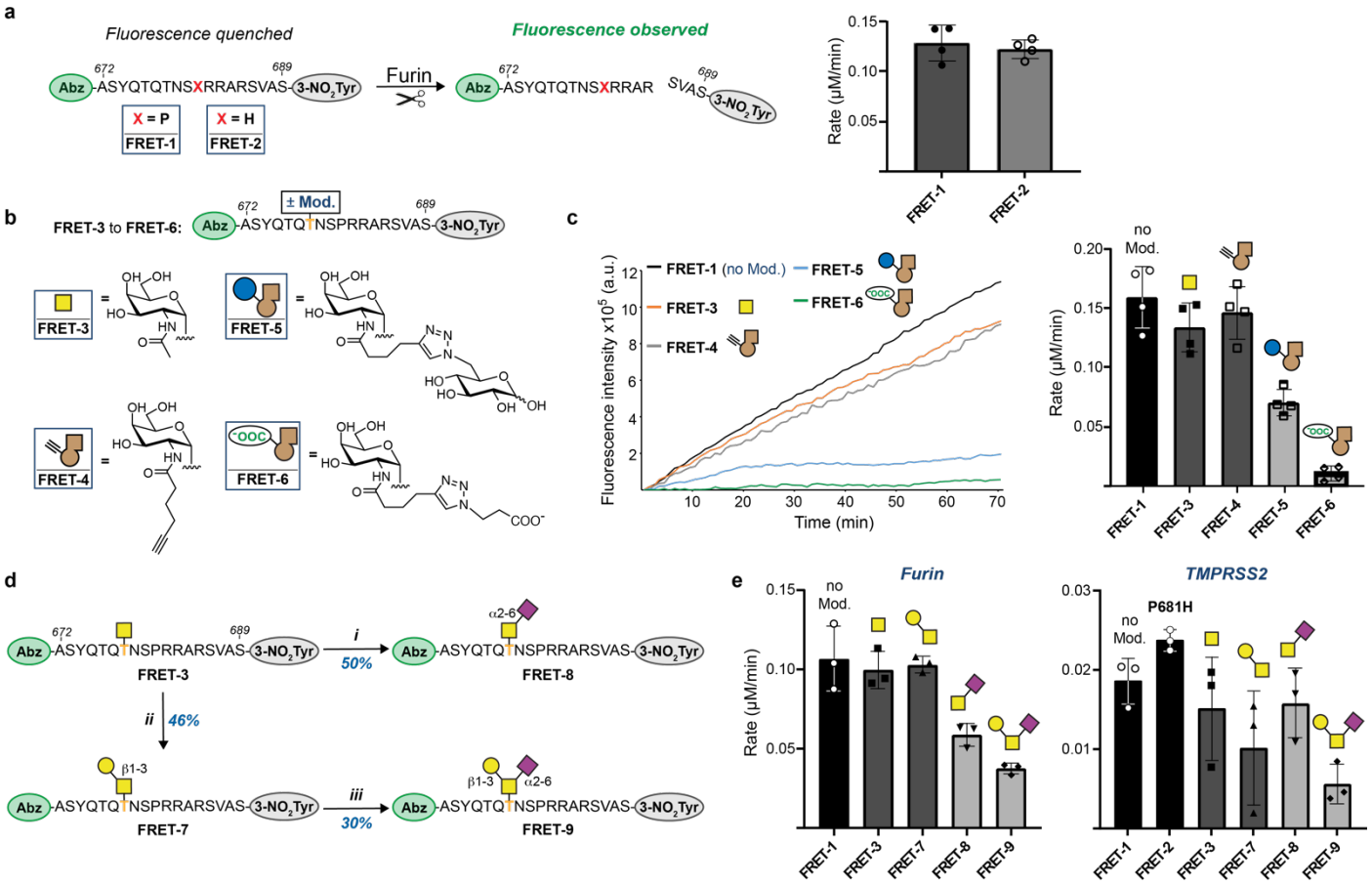

Figure 5. Chemical elaboration of *O*-glycosylation impacts proteolytic cleavage. **a)** Experimental design and comparison of furin cleavage between WT and P681H peptide substrates. Peptides containing N-terminal 2-aminobenzoate (Abz) as a FRET donor, and C-terminal 3-nitrotyrosine (3-NO_2Tyr) as a FRET quencher that was removed upon furin cleavage. **b)** Chemical modifications of synthetic (glyco)peptides **FRET-3** through **FRET-6**, generated via in vitro glycosylation and CuAAC. **c)** Left: Time course of fluorescence increase upon furin cleavage reactions of 20 µM **FRET-1** and **FRET-3** to **FRET-6** with 0.8 U/mL furin. Linear fluorescence increase is shown and normalized to the corresponding control run without furin. Right: Rates of furin cleavage of glycopeptides **FRET-1** and **FRET-3** to **FRET-6** obtained through linear regression and normalization to control runs without furin. Data are means +SD of four independent experiments. **d)** Chemoenzymatic synthesis of glycopeptides **FRET-7** through **FRET-9:** *i.* ST6GalNAc-1 (150 µg/mL), CMP-Neu5Ac (1.5 eq.), pH 7.5, 37°C for 16 hours, 46% yield; *ii. Dm*C1GalT1 (1 µM), UDP-Gal (1.5 eq.), pH 7.5, 37°C for 16 hours, 50% yield; *iii.* ST6GALNAC-2 (10 µg/mL), CMP-Neu5Ac (1.5 eq.), pH 7.5, 37°C for 48 hours, 30% yield. **e)** Rates of furin and TMPRSS cleavage of (glyco)peptides **FRET-1** to **FRET-3** and **FRET-7** to **FRET-9** obtained through linear regression and normalization to control runs without furin. Data are means +SD of three independent experiments**.** CMP = cytidine monophosphate; CIAP = Calf intestinal alkaline phosphatase.

Our *in vitro* glycosylation experiments of recombinant WT spike suggested that only S1 is a major substrate for GalNAc-T1 after secretion from human cells (**Figure 2b**). Such behaviour could be explained by the presence of elaborated, sialylated *O*-glycans on recombinantly expressed FL-S, which would both prevent furin cleavage and block access to GalNAc-T1 *in vitro*. This would suggest a relative enrichment of sialylated

O-glycans on FL-S but not S1. To test this notion, we subjected both FL-S and S1/S2 gel bands from a recombinant spike preparation to MS-glycoproteomics analysis, then analysed the data for both simple and elaborated *O*-GalNAc glycans. By calculating the intact masses of various expected *O*-glycopeptides in recombinant spike and then obtaining the associated extracted ion chromatograms (XICs), we found that over 5-fold higher glycopeptide signal is present in FL-S when compared to cleaved S1/S2 fractions (**Figure 6**). Furthermore, when only accounting for sialic acid-containing glycopeptides, an ~8-fold higher abundance was observed for FL-S when compared to S1/S2.

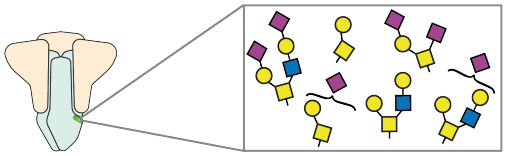

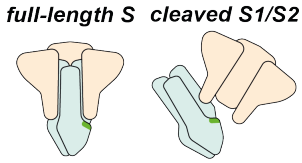

Peptide Sequence (662–682)	Glycan	$[M+H]^+$	Mass Area (full-length S)	Mass Area (cleaved S1/S2)
CDIPIGAGICASYQTQTNSPR	HexNAc(2)Hex(2)NeuAc(2)	3621.5200	2.8742	not found
CDIPIGAGICASYQTQTNSPR	HexNAc(2)Hex(2)NeuAc(1)	3330.4238	4.0709	not found
CDIPIGAGICASYQTQTNSPR	HexNAc(1)Hex(1)NeuAc(2)	3256.3870	5.0207	1.0136
CDIPIGAGICASYQTQTNSPR	HexNAc(1)Hex(1)NeuAc(1)	2965.2920	3.2551	0.8252
CDIPIGAGICASYQTQTNSPR	HexNAc(2)Hex(2)	3039.3276	4.0210	0.2453
CDIPIGAGICASYQTQTNSPR	HexNAc(1)Hex(1)	2674.1958	9.5992	3.0845
		Total	28.8411	5.1686

5.6x

Figure 6. XICs for *O*-glycopeptides from FL-I-S or S1/S2 recombinant spike fractions. Mass areas were normalised against their corresponding base peaks and multiplied by a factor of 10,000. All data analysis was performed in Thermo XCalibur software and hand-curated.

DISCUSSION

Our data strongly indicate that elaborated, negatively charged *O*-GalNAc glycans on Thr678 of SARS-CoV-2 spike have a detrimental effect on furin cleavage. Such glycans are produced on lung epithelial cells that express GalNAc-T1,[73] suggesting that glycosylation is a physiologically relevant modification that could restrict the maturation of spike in WT SARS-CoV-2.[96] The propensity of SARS-CoV-2 variants of concern to outcompete each other has been linked to both increased infectivity and immune escape. Within the evolutionary trajectory from the alpha to delta and omicron variants, notable changes in the amino acid sequence proximal to the FCS indicated that proteolytic cleavage is gradually enhanced, congruent with their increased infectivity. Mutations of Pro681 have been detected in early variants such as Alpha (P681H). We found that this mutation did not increase the rate of cleavage by both furin and TMPRSS2, placing further emphasis on glycosylation as a restricting factor for spike maturation. Notably, the analogous mutation found on the more transmissible Delta variant (P681R) has been linked to an increase in furin cleavage by Whittaker and colleagues,[43] suggesting an evolutionary trajectory that places suppression of *O*-glycosylation before increasing intrinsic furin recognition. This is further underlined by the mutations found in Omicron, combining the P681H with the N679K mutation: In contrast to P681H and consistent with mapped amino acid preferences of GalNAc-T1,[97] the N679K mutation does not substantially impact glycosylation, but it leads to enhanced furin cleavage of synthetic peptides.[43] These FCS-adjacent mutations therefore act synergistically and have likely evolved to both suppress glycosylation and intrinsically enhance furin cleavage. Since the closest relatives to SARS-CoV-2, the strains RaTG13 Bat-CoV and GD Pangolin-CoV, share the exact same

peptide sequence without harbouring an FCS (**Figure 1**), we speculate that *O*-glycosylation might have been a remnant of ancestral strains that is being subsequently lost through viral evolution.

The presence of *O*-GalNAc glycans immediately adjacent to proteolytic cleavage sites has been found to impact processing of secreted proteins.[74–78] The glycosylation site at Thr678 of spike is not in direct proximity to the FCS, explaining why a single GalNAc residue is not sufficient to modulate furin activity while only slightly impacting TMPRSS2 activity. Instead, elaboration and sialylation negatively impact the cleavage rates, further highlighting the need for accurate glycan tracing techniques.[98] Tuning the chemical properties of glycopeptides in a straightforward fashion by CuAAC was crucial to gain an initial understanding of the substrate-activity relationship of proteases. This strategy informed the targeted synthesis of elaborated *O*-glycopeptide substrates, providing a convenient method to fine-tune substrate scope in a time- and resource-efficient manner. Chemical tools thus provided insights into glycosyltransferase specificity, detectability by mass spectrometry, and protease substrate specificity, showcasing the power of such tools in biomedical discovery.

AUTHOR INFORMATION

Corresponding Author

*b.schumann@imperial.ac.uk

ACKNOWLEDGMENTS

We thank David Briggs, Sarah Maslen, Neil McDonald, Phil Walker, Steve Gamblin and Nicola O'Reilly for valuable support and Theresa Zeisner, Jennifer Milligan and John Diffley for helpful discussions. We thank Kelly Ten Hagen and Nadine Samara for providing crucial insight. We thank Junwon Choi and Carolyn R. Bertozzi for UDP-GalN6yne. This work was supported by the Francis Crick Institute which receives its core funding from Cancer Research UK (FC001749 and FC0010219), the UK Medical Research Council (FC001749 and FC0010219), and the Wellcome Trust (FC001749 and FC0010219). This work was funded by the UK Biotechnology and Biological Sciences Research Council (BB/V008439/1 to E. G.-R., L. D. V. and B. S., BB/V014862/1 to G. B.-T. and B. S. and BB/M028836/1 to S. L. F.), the Engineering and Physical Sciences Research Council (EP/S005226/1 to S. L. F.), the Wellcome Trust (218304/Z/19/Z to A. M. and B. S.) and the European Research Council (788231 to S. L. F.). M. Z.-H. was supported by a Crick-HEI studentship funded by the Department of Chemistry at Imperial College London and the Francis Crick Institute. S. A. M. is supported by the Yale Science Development Fund and NIGMS R35 GM147039. K. E. M. is supported by a Yale Endowed Postdoctoral Fellowship. R.J.W. receives support from Rosetrees (M926). R.H.-G., thanks ARAID, the Agencia Estatal de Investigación (AEI, BFU2016-75633-P and PID2019-105451GB-I00) and Gobierno de Aragón (E34_R17 and LMP58_18 to R.H.-G.) with FEDER (2014–2020) funds for "Building Europe from Aragón" for financial support. For the purposes of Open access, the author has applied a CC-BY copyright to any author accepted version of a manuscript arising from this submission.

REFERENCES

1. Hoffmann, M. *et al.* SARS-CoV-2 Cell Entry Depends on ACE2 and TMPRSS2 and Is Blocked by a Clinically Proven Protease Inhibitor. *Cell* **181**, 271-280.e8 (2020).

2. Moreira, R. A., Guzman, H. V., Boopathi, S., Baker, J. L. & Poma, A. B. Characterization of structural and energetic differences between conformations of the SARS-CoV-2 spike protein. *Materials (Basel).* **13**, 1–14 (2020).

3. Benton, D. J. *et al.* Receptor binding and priming of the spike protein of SARS-CoV-2 for membrane fusion. *Nature* **588**, 327–330 (2020).

4. Wrobel, A. G. *et al.* Structure and binding properties of Pangolin-CoV spike glycoprotein inform the evolution of SARS-CoV-2. *Nat. Commun. 2021 121* **12**, 1–6 (2021).

5. Benton, D. J. *et al.* The effect of the D614G substitution on the structure of the spike glycoprotein of SARS-CoV-2. *Proc. Natl. Acad. Sci. U. S. A.* **118**, (2021).

6. Turoňová, B. *et al.* In situ structural analysis of SARS-CoV-2 spike reveals flexibility mediated by three hinges. *Science* **370**, 203–208 (2020).

7. Shang, J. *et al.* Cell entry mechanisms of SARS-CoV-2. *Proc. Natl. Acad. Sci. U. S. A.* **117**, 11727–11734 (2020).

8. Yang, J. *et al.* Molecular interaction and inhibition of SARS-CoV-2 binding to the ACE2 receptor. *Nat. Commun.* **11**, 1–10 (2020).

9. Wrapp, D. *et al.* Cryo-EM structure of the 2019-nCoV spike in the prefusion conformation. *Science* **367**, 1260–1263 (2020).

10. Hsieh, C. L. *et al.* Structure-based design of prefusion-stabilized SARS-CoV-2 spikes. *Science* **369**, 1501–1505 (2020).

11. Cai, Y. *et al.* Distinct conformational states of SARS-CoV-2 spike protein. *Science* **369**, 1586–1592 (2020).

12. Yan, R. *et al.* Structural basis for the recognition of SARS-CoV-2 by full-length human ACE2. *Science* **367**, 1444–1448 (2020).

13. Yu, A. *et al.* A multiscale coarse-grained model of the SARS-CoV-2 virion. *Biophys. J.* **120**, 1097–1104 (2021).

14. Wrobel, A. G. *et al.* SARS-CoV-2 and bat RaTG13 spike glycoprotein structures inform on virus evolution and furin-cleavage effects. *Nat. Struct. Mol. Biol.* **27**, 763–767 (2020).

15. Shajahan, A., Supekar, N. T., Gleinich, A. S. & Azadi, P. Deducing the N- and O-glycosylation profile

of the spike protein of novel coronavirus SARS-CoV-2. *Glycobiology* **30**, 981–988 (2020).

16. Rosenbalm, K. E., Tiemeyer, M., Wells, L., Aoki, K. & Zhao, P. Glycomics-informed glycoproteomic analysis of site-specific glycosylation for SARS-CoV-2 spike protein. *STAR Protoc.* **1**, 100214 (2020).

17. Zhang, Y. *et al.* O-Glycosylation Landscapes of SARS-CoV-2 Spike Proteins. *Front. Chem.* **9**, 729 (2021).

18. Harbison, A. M. *et al.* Fine-tuning the Spike: Role of the nature and topology of the glycan shield in the structure and dynamics of SARS-CoV-2 S. *bioRxiv* 2021.04.01.438036 (2021) doi:10.1101/2021.04.01.438036.

19. Gong, Y., Qin, S., Dai, L. & Tian, Z. The glycosylation in SARS-CoV-2 and its receptor ACE2. *Signal Transduct. Target. Ther. 2021 61* **6**, 1–24 (2021).

20. Allen, J. D. *et al.* Site-Specific Steric Control of SARS-CoV-2 Spike Glycosylation. *Biochemistry* **60**, 2153–2169 (2021).

21. Xu, W., Wang, M., Yu, D. & Zhang, X. Variations in SARS-CoV-2 Spike Protein Cell Epitopes and Glycosylation Profiles During Global Transmission Course of COVID-19. *Front. Immunol.* **11**, 2222 (2020).

22. Watanabe, Y., Allen, J. D., Wrapp, D., McLellan, J. S. & Crispin, M. Site-specific glycan analysis of the SARS-CoV-2 spike. *Science* **369**, 330–333 (2020).

23. Grant, O. C., Montgomery, D., Ito, K. & Woods, R. J. Analysis of the SARS-CoV-2 spike protein glycan shield reveals implications for immune recognition. *Sci. Rep.* **10**, 14991 (2020).

24. Casalino, L. *et al.* Beyond shielding: The roles of glycans in the SARS-CoV-2 spike protein. *ACS Cent. Sci.* **6**, 1722–1734 (2020).

25. Yang, Q. *et al.* Inhibition of SARS-CoV-2 viral entry upon blocking N-and O-glycan elaboration. *Elife* **9**, 1–44 (2020).

26. Gao, C. *et al.* SARS-CoV-2 Spike Protein Interacts with Multiple Innate Immune Receptors. *bioRxiv Prepr. Serv. Biol.* 2020.07.29.227462 (2020) doi:10.1101/2020.07.29.227462.

27. Sanda, M., Morrison, L. & Goldman, R. N-and O-Glycosylation of the SARS-CoV-2 Spike Protein. *Anal. Chem.* **93**, 2003–2009 (2021).

28. Sztain, T. *et al.* A glycan gate controls opening of the SARS-CoV-2 spike protein. *Nat. Chem. 2021 1310* **13**, 963–968 (2021).

29. Wrobel, A. G. *et al.* SARS-CoV-2 and bat RaTG13 spike glycoprotein structures inform on virus evolution and furin-cleavage effects. *Nat. Struct. Mol. Biol. 2020 278* **27**, 763–767 (2020).

30. Pak, A. J., Yu, A., Ke, Z., Briggs, J. A. G. & Voth, G. A. Cooperative multivalent receptor binding promotes exposure of the SARS-CoV-2 fusion machinery core. *Nat. Commun. 2022 131* **13**, 1–12 (2022).

31. Hoffmann, M., Kleine-Weber, H. & Pöhlmann, S. A Multibasic Cleavage Site in the Spike Protein of SARS-CoV-2 Is Essential for Infection of Human Lung Cells. *Mol. Cell* **78**, 779-784.e5 (2020).

32. Coutard, B. *et al.* The spike glycoprotein of the new coronavirus 2019-nCoV contains a furin-like cleavage site absent in CoV of the same clade. *Antiviral Res.* **176**, 104742 (2020).

33. Örd, M., Faustova, I. & Loog, M. The sequence at Spike S1/S2 site enables cleavage by furin and phospho-regulation in SARS-CoV2 but not in SARS-CoV1 or MERS-CoV. *Sci. Reports 2020 101* **10**, 1–10 (2020).

34. Xia, S. *et al.* The role of furin cleavage site in SARS-CoV-2 spike protein-mediated membrane fusion in the presence or absence of trypsin. *Signal Transduct. Target. Ther. 2020 51* **5**, 1–3 (2020).

35. Bestle, D. *et al.* TMPRSS2 and furin are both essential for proteolytic activation of SARS-CoV-2 in human airway cells. *Life Sci. Alliance* **3**, (2020).

36. Whittaker, G. R. SARS-CoV-2 spike and its adaptable furin cleavage site. *The Lancet Microbe* **2**, e488–e489 (2021).

37. Peacock, T. P. *et al.* The furin cleavage site in the SARS-CoV-2 spike protein is required for transmission in ferrets. *Nat. Microbiol. 2021 67* **6**, 899–909 (2021).

38. Johnson, B. A. *et al.* Loss of furin cleavage site attenuates SARS-CoV-2 pathogenesis. *Nat. 2021 5917849* **591**, 293–299 (2021).

39. Papa, G. *et al.* Furin cleavage of SARS-CoV-2 Spike promotes but is not essential for infection and cell-cell fusion. *PLOS Pathog.* **17**, e1009246 (2021).

40. Essalmani, R. *et al.* Distinctive Roles of Furin and TMPRSS2 in SARS-CoV-2 Infectivity. *J. Virol.* **96**, (2022).

41. Lucas, J. M. *et al.* The androgen-regulated protease TMPRSS2 activates a proteolytic cascade involving components of the tumor microenvironment and promotes prostate cancer metastasis. *Cancer Discov.* **4**, 1310–1325 (2014).

42. Liu, Y. *et al.* Delta spike P681R mutation enhances SARS-CoV-2 fitness over Alpha variant. *Cell Rep.* **39**, (2022).

43. Lubinski, B., Jaimes, J. A. & Whittaker, G. R. Intrinsic furin-mediated cleavability of the spike S1/S2 site from SARS-CoV-2 variant B.1.529 (Omicron). *bioRxiv* 2022.04.20.488969 (2022) doi:10.1101/2022.04.20.488969.

44. Peacock, T. P. *et al.* The furin cleavage site of SARS-CoV-2 spike protein is a key determinant for transmission due to enhanced replication in airway cells. *bioRxiv* 2020.09.30.318311 (2020) doi:10.1101/2020.09.30.318311.

45. Wrobel, A. G. *et al.* Evolution of the SARS-CoV-2 spike protein in the human host. *Nat. Commun. 2022 131* **13**, 1–7 (2022).

46. Schjoldager, K. T., Narimatsu, Y., Joshi, H. J. & Clausen, H. Global view of human protein glycosylation pathways and functions. *Nat. Rev. Mol. Cell Biol. 2020 2112* **21**, 729–749 (2020).

47. Čaval, T., de Haan, N., Konstantinidi, A. & Vakhrushev, S. Y. Quantitative characterization of O-GalNAc glycosylation. *Curr. Opin. Struct. Biol.* **68**, 135–141 (2021).

48. Kotwal, G. J. *et al.* Role of Glycosylation in Transport of Vesicular Stomatitis Virus Envelope Glycoprotein A NEW CLASS OF MUTANT DEFECTIVE IN GLYCOSYLATION AND TRANSPORT OF G PROTEIN*. *J. Biol. Chem.* **261**, 8936–8943 (1986).

49. Chernykh, A., Kawahara, R. & Thaysen-Andersen, M. Towards structure-focused glycoproteomics. *Biochem. Soc. Trans.* **49**, 161–186 (2021).

50. Yu, A. *et al.* Advances in mass spectrometry-based glycoproteomics. *Electrophoresis* **39**, 3104–3122 (2018).

51. Chen, Z., Huang, J. & Li, L. Recent advances in mass spectrometry (MS)-based glycoproteomics in complex biological samples. *TrAC Trends Anal. Chem.* **118**, 880–892 (2019).

52. Abrahams, J. L. *et al.* Recent advances in glycoinformatic platforms for glycomics and glycoproteomics. *Curr. Opin. Struct. Biol.* **62**, 56–69 (2020).

53. Khoo, K. H. Advances toward mapping the full extent of protein site-specific O-GalNAc glycosylation that better reflects underlying glycomic complexity. *Curr. Opin. Struct. Biol.* **56**, 146–154 (2019).

54. Malaker, S. A. *et al.* The mucin-selective protease StcE enables molecular and functional analysis of human cancer-associated mucins. *Proc. Natl. Acad. Sci. U. S. A.* **116**, 7278–7287 (2019).

55. Rangel-Angarita, V. & Malaker, S. A. Mucinomics as the Next Frontier of Mass Spectrometry. *ACS Chem. Biol.* **16**, 1866–1883 (2021).

56. Cioce, A., Malaker, S. A. & Schumann, B. Generating orthogonal glycosyltransferase and nucleotide sugar pairs as next-generation glycobiology tools. *Current Opinion in Chemical Biology* vol. 60 66–78 (2021).

57. Zhang, L. *et al.* Furin cleavage of the SARS-CoV-2 spike is modulated by O-glycosylation. *Proc. Natl. Acad. Sci. U. S. A.* **118**, 2109905118 (2021).

58. Steentoft, C. *et al.* Precision mapping of the human O-GalNAc glycoproteome through SimpleCell technology. *EMBO J.* **32**, 1478–1488 (2013).

59. Ten Hagen, K. G., Fritz, T. A. & Tabak, L. A. All in the family: the UDP-GalNAc:polypeptide N-acetylgalactosaminyltransferases. *Glycobiology* **13**, 1R-16R (2003).

60. Revoredo, L. *et al.* Mucin-type O-glycosylation is controlled by short- and long-range glycopeptide substrate recognition that varies among members of the polypeptide GalNAc transferase family. *Glycobiology* **26**, 360–376 (2016).

61. Gerken, T. A. *et al.* Emerging paradigms for the initiation of mucin-type protein O-glycosylation by the

polypeptide GalNAc transferase family of glycosyltransferases. *J. Biol. Chem.* **286**, 14493–14507 (2011).

62. Becker, J. L., Tran, D. T. & Tabak, L. A. Members of the GalNAc-T family of enzymes utilize distinct Golgi localization mechanisms. *Glycobiology* **28**, 841–848 (2018).

63. Gerken, T. A. *et al.* The Lectin Domain of the Polypeptide GalNAc Transferase Family of Glycosyltransferases (ppGalNAc Ts) Acts as a Switch Directing Glycopeptide Substrate Glycosylation in an N- or C-terminal Direction, Further Controlling Mucin Type O-Glycosylation *. *J. Biol. Chem.* **288**, 19900–19914 (2013).

64. Beaman, E.-M., Carter, D. R. F. & Brooks, S. A. GALNTs: master regulators of metastasis-associated epithelial-mesenchymal transition (EMT)? *Glycobiology* (2022) doi:10.1093/GLYCOB/CWAC014.

65. Wandall, H. H., Nielsen, M. A. I., King-Smith, S., Haan, N. & Bagdonaite, I. Global functions of O-glycosylation: promises and challenges in O-glycobiology. *FEBS J.* febs.16148 (2021) doi:10.1111/FEBS.16148.

66. Pratt, M. R. *et al.* Deconvoluting the Functions of Polypeptide N-α-Acetylgalactosaminyltransferase Family Members by Glycopeptide Substrate Profiling. *Chem. Biol.* **11**, 1009–1016 (2004).

67. Bennett, E. P. *et al.* Control of mucin-type O-glycosylation: A classification of the polypeptide GalNAc-transferase gene family. *Glycobiology* **22**, 736–756 (2012).

68. Narimatsu, Y. *et al.* Exploring regulation of protein O-glycosylation in isogenic human HEK293 cells by differential O-glycoproteomics. *Mol. Cell. Proteomics* **18**, 1396–1409 (2019).

69. Narimatsu, Y. *et al.* Exploring Regulation of Protein O-Glycosylation in Isogenic Human HEK293 Cells by Differential O-Glycoproteomics. *Mol. Cell. Proteomics* **18**, 1396–1409 (2019).

70. Steentoft, C. *et al.* Mining the O-glycoproteome using zinc-finger nuclease–glycoengineered SimpleCell lines. *Nat. Methods 2011 811* **8**, 977–982 (2011).

71. Schjoldager, K. T. B. G. *et al.* Probing isoform-specific functions of polypeptide GalNAc-transferases using zinc finger nuclease glycoengineered SimpleCells. *Proc. Natl. Acad. Sci. U. S. A.* **109**, 9893–9898 (2012).

72. Vakhrushev, S. Y. *et al.* Enhanced mass spectrometric mapping of the human GalNAc-type O-glycoproteome with simplecells. *Mol. Cell. Proteomics* **12**, 932–944 (2013).

73. Zhang, L. *et al.* Furin cleavage of the SARS-CoV-2 spike is modulated by O-glycosylation. *Biorxiv* (2021) doi:10.1101/2021.02.05.429982.

74. Schjoldager, K. T. B. G. *et al.* A Systematic Study of Site-specific GalNAc-type O-Glycosylation Modulating Proprotein Convertase Processing. *J. Biol. Chem.* **286**, 40122–40132 (2011).

75. Kozarsky, K., Kingsley, D. & Krieger, M. Use of a mutant cell line to study the kinetics and function of O-linked glycosylation of low density lipoprotein receptors. *Proc. Natl. Acad. Sci. U. S. A.* **85**, 4335–4339 (1988).

76. Kato, K. *et al.* Polypeptide GalNAc-transferase T3 and Familial Tumoral Calcinosis: SECRETION OF FIBROBLAST GROWTH FACTOR 23 REQUIRES O-GLYCOSYLATION. *J. Biol. Chem.* **281**, 18370–18377 (2006).

77. Schjoldager, K. T. B. G. *et al.* O-glycosylation modulates proprotein convertase activation of angiopoietin-like protein 3: Possible role of polypeptide GalNAc-transferase-2 in regulation of concentrations of plasma lipids. *J. Biol. Chem.* **285**, 36293–36303 (2010).

78. Tagliabracci, V. S. *et al.* Dynamic regulation of FGF23 by Fam20C phosphorylation, GalNAc-T3 glycosylation, and furin proteolysis. *Proc. Natl. Acad. Sci. U. S. A.* **111**, 5520–5525 (2014).

79. Choi, J. *et al.* Engineering Orthogonal Polypeptide GalNAc-Transferase and UDP-Sugar Pairs. *J. Am. Chem. Soc.* **141**, 13442–13453 (2019).

80. Schumann, B. *et al.* Bump-and-Hole Engineering Identifies Specific Substrates of Glycosyltransferases in Living Cells. *Mol. Cell* **78**, 824-834.e15 (2020).

81. Cioce, A., Malaker, S. A. & Schumann, B. Generating orthogonal glycosyltransferase and nucleotide sugar pairs as next-generation glycobiology tools. *Curr. Opin. Chem. Biol.* **60**, 66–78 (2021).

82. Cioce, A. *et al.* Optimization of Metabolic Oligosaccharide Engineering with Ac4GalNAlk and Ac4GlcNAlk by an Engineered Pyrophosphorylase. *ACS Chem. Biol.* **16**, 1961–1967 (2021).

83. Cioce, A. *et al.* Cell-specific Bioorthogonal Tagging of Glycoproteins. *bioRxiv* 2021.07.28.454135 (2021) doi:10.1101/2021.07.28.454135.

84. Calle, B. *et al.* Benefits of Chemical Sugar Modifications Introduced by Click Chemistry for Glycoproteomic Analyses. *J. Am. Soc. Mass Spectrom.* **32**, 2366–2375 (2021).

85. Song, K.-H. *et al.* GALNT14 promotes lung-specific breast cancer metastasis by modulating self-renewal and interaction with the lung microenvironment. *Nat. Commun. 2016 71* **7**, 1–15 (2016).

86. de las Rivas, M., Lira-Navarrete, E., Gerken, T. A. & Hurtado-Guerrero, R. Polypeptide GalNAc-Ts: from redundancy to specificity. *Current Opinion in Structural Biology* vol. 56 87–96 (2019).

87. Cioce, A. *et al.* Cell-specific Bioorthogonal Tagging of Glycoproteins in Co-culture. *bioRxiv* 2021.07.28.454135 (2021) doi:10.1101/2021.07.28.454135.

88. Sittel, I. & Galan, M. C. Chemo-enzymatic synthesis of imidazolium-tagged sialyllactosamine probes. *Bioorg. Med. Chem. Lett.* **25**, 4329–4332 (2015).

89. Sittel, I. & Galan, M. C. Imidazolium-labeled glycosides as probes to harness glycosyltransferase activity in human breast milk. *Org. Biomol. Chem.* **15**, 3575–3579 (2017).

90. Sittel, I., Tran, A. T., Benito-Alifonso, D. & Galan, M. C. Combinatorial ionic catch-and-release oligosaccharide synthesis (combi-ICROS). *Chem. Commun.* **49**, 4217–4219 (2013).

91. Riley, N. M., Malaker, S. A. & Bertozzi, C. R. Electron-Based Dissociation Is Needed for O-Glycopeptides Derived from OpeRATOR Proteolysis. *Anal. Chem.* **92**, 14878–14884 (2020).

92. Riley, N. M., Malaker, S. A., Driessen, M. D. & Bertozzi, C. R. Optimal Dissociation Methods Differ for N- A nd O-Glycopeptides. *J. Proteome Res.* **19**, 3286–3301 (2020).

93. Lim, C. T. *et al.* Identifying SARS-CoV-2 antiviral compounds by screening for small molecule inhibitors of Nsp3 papain-like protease. *Biochem. J.* **478**, 2517–2531 (2021).

94. González-Ramírez, A. M. *et al.* Structural basis for the synthesis of the core 1 structure by C1GalT1. *Nat. Commun.* **13**, (2022).

95. Zong, G. *et al.* A facile chemoenzymatic synthesis of SARS-CoV-2 glycopeptides for probing glycosylation functions. *Chem. Commun.* **57**, 6804–6807 (2021).

96. Jia, N. *et al.* The Human Lung Glycome Reveals Novel Glycan Ligands for Influenza A Virus. *Sci. Reports 2020 101* **10**, 1–14 (2020).

97. Gerken, T. A. *et al.* Emerging Paradigms for the Initiation of Mucin-type Protein O-Glycosylation by the Polypeptide GalNAc Transferase Family of Glycosyltransferases. *J. Biol. Chem.* **286**, 14493–14507 (2011).

98. Jiang, J., Pristera, N., Wang, W., Zhang, X. & Wu, Q. Effect of Sialylated O-Glycans in Pro–Brain Natriuretic Peptide Stability. *Clin. Chem.* **56**, 959–966 (2010).